# Solution of Linear Systems in Fourier-Based Methods for Aircraft Applications

A. McCracken[†], A. Da Ronch[‡], S. Timme[§], K. J. Badcock[¶]
School of Engineering, University of Liverpool, Liverpool, L69 3GH, United Kingdom

Computational fluid dynamics Fourier-based methods have found increasing use for aircraft applications in the last decade. Two applications which benefit are aeroelastic stability analysis and flight dynamics for which previous work is reviewed here. The implicit solution of the methods considered in this work, require an effective preconditioner for solving the linear systems. New results are presented to understand the performance of an approach to accelerate the convergence of the linear solver. The computational performance of the resulting solver is considered for flutter and dynamic derivative calculations.

**Keywords:** Frequency Domain Methods; Linear Frequency Domain; Harmonic Balance; Aeroelasticity; Flight Dynamics; ILU Preconditioning

## 1. Introduction

Unsteady flow problems encountered for aircraft applications can involve a periodic oscillation, allowing the use of Fourier-based methods. These methods can reduce the computational time significantly due to direct calculation of the periodic state rather than computing the transient response. The development of Fourier-based methods has largely been for the analysis of turbomachinery flows with the two methods used here, namely Linear Frequency Domain and Harmonic Balance, having their roots in this field. Hall and Crawley (1989) proposed a linearised Euler method where the equations were linearised about a steady mean state with a small perturbation for the analysis of a flutter and a gust-response problem for a turbomachinery cascade flow. This approach was extended to capture non-linearities, and subsequently for the Navier-Stokes equations in He and Ning (1998).

The Harmonic Balance method was developed for unsteady nonlinear turbomachinery flows in Hall *et al.* (2002) and used in Thomas *et al.* (2002) and Thomas *et al.* (2004) for aeroelastic analysis in the transonic regime for both inviscid and viscous flows. A similar

[†]PhD Student, corresponding author, A.J.McCracken@liverpool.ac.uk
[‡]Research Associate
[§]Research Associate
[¶]Professor

method presented in McMullen *et al.* (2006) solves the system in the frequency domain with a specified number of retained harmonics rather than the solution taking place in the time domain.

Fourier-based methods are finding increasing use for external aircraft problems. Two applications that can benefit include aeroelasticity (e.g. Mortchelewicz (1998)) and for the calculation of dynamic stability derivatives of rigid aircraft (e.g. Murman (2007), Da Ronch *et al.* (2011b) and Mialon *et al.* (2011)).

This paper continues with a brief description of the formulation of the two frequency domain methods used here before moving to a discussion of the main numerical challenge involved in solving linear systems. Two applications of Fourier-based methods for external aerodynamic problems are then reviewed, before concluding with an evaluation of when these methods are especially useful.

## 2. Formulation

### 2.1. *Linear Frequency Domain*

The governing equations of a fluid flow are first written in the semi-discrete form,

$$\frac{\mathrm{d}\mathbf{w}}{\mathrm{d}t} + \mathbf{R}(\mathbf{w}, \mathbf{u}, \dot{\mathbf{u}}) = \mathbf{0}, \tag{1}$$

where $\mathbf{R}$ is the fluid residual and $\mathbf{w}$ is the flow solution. The fluid residual is influenced by the structural motion (described by the unknowns $\mathbf{u}$ and $\dot{\mathbf{u}}$) due to boundary conditions applied at the interface between the fluid and structure. Also, the surface deformations and velocities are communicated to the volume mesh giving the dependences on $\mathbf{u}$ and $\dot{\mathbf{u}}$.

The basis of the linear frequency domain (LFD) method is the assumption of small amplitudes which allows the variables to be represented as a small perturbation about a steady mean state. This gives rise to

$$\mathbf{w}(\mathbf{t}) = \bar{\mathbf{w}} + \tilde{\mathbf{w}}(\mathbf{t}), \quad \mathbf{u}(\mathbf{t}) = \bar{\mathbf{u}} + \tilde{\mathbf{u}}(\mathbf{t}). \tag{2}$$

The small time-dependent perturbation is assumed to be periodic which is then written as a Fourier series in terms of the base frequency $\omega$. This is combined with Eqs. (1) and (2) to give,

$$\left\{ in\omega I + \frac{\partial \mathbf{R}}{\partial \mathbf{w}} \right\} \hat{\mathbf{w}}_n = -\frac{\partial \mathbf{R}}{\partial \mathbf{u}} \hat{\mathbf{u}}_n - in\omega \frac{\partial \mathbf{R}}{\partial \dot{\mathbf{u}}} \hat{\mathbf{u}}_n. \tag{3}$$

where the hat accent indicates a vector of Fourier coefficients i.e. the sine and cosine terms for each harmonic. Limiting interest to the first harmonic of the Fourier series, $n$ is taken to be 1, and hence the nonlinear Eq. (1) has been reduced to a single linear equation in the frequency domain. The linear system is then solved for the Fourier coefficients of the flow solution $\hat{\mathbf{w}}$.

Equation (3) is a complex-valued linear system which can either be solved using complex arithmetic or represented as two coupled real systems. For the latter, the real and imaginary parts, with subscripts Re and Im, are written in the form $\mathbf{Ax} = \mathbf{b}$ where,

$$\mathbf{A} = \begin{bmatrix} \frac{\partial \mathbf{R}}{\partial \mathbf{w}} & -\omega \mathbf{I} \\ \omega \mathbf{I} & \frac{\partial \mathbf{R}}{\partial \mathbf{w}} \end{bmatrix}, \quad \mathbf{x} = \begin{pmatrix} \hat{\mathbf{w}}_{Re} \\ \hat{\mathbf{w}}_{Im} \end{pmatrix}, \text{ and } \mathbf{b} = \begin{bmatrix} -\frac{\partial \mathbf{R}}{\partial \mathbf{u}} & \omega \frac{\partial \mathbf{R}}{\partial \dot{\mathbf{u}}} \\ -\omega \frac{\partial \mathbf{R}}{\partial \dot{\mathbf{u}}} & -\frac{\partial \mathbf{R}}{\partial \mathbf{u}} \end{bmatrix} \begin{pmatrix} \hat{\mathbf{u}}_{Re} \\ \hat{\mathbf{u}}_{Im} \end{pmatrix}. \tag{4}$$

## 2.2. *Harmonic Balance*

The Harmonic Balance (HB) technique was proposed in Hall *et al.* (2002) for use with turbo-machinery flows. Unlike LFD, the system is never linearised but instead takes the semi-discrete flow equations (1), using the assumption of periodicity to model the flow variables and residuals as a Fourier series with frequency $\omega$, and truncated to a specified number of harmonics $N_H$,

$$\mathbf{w(t)} \approx \hat{\mathbf{w}}_\mathbf{0} + \sum_{\mathbf{n=1}}^{\mathbf{N_H}} \big( \hat{\mathbf{w}}_{\mathbf{a_n}} \cos(\omega \mathbf{nt}) + \hat{\mathbf{w}}_{\mathbf{b_n}} \sin(\omega \mathbf{nt}) \big). \tag{5}$$

Combining Eqs. (1) and (5), then grouping similar harmonic terms gives a system of $N_T = 2N_H + 1$ equations, written in matrix form as,

$$\omega \mathbf{A} \hat{\mathbf{w}} + \hat{\mathbf{R}} = \mathbf{0}, \tag{6}$$

where $\mathbf{A}$ is an $N_T \times N_T$ matrix containing terms $\mathbf{A}$(n+1,$N_H$+n+1) = n and $\mathbf{A}$($N_H$+n+1,n+1) = -n.

The solution of the system is discretised into $N_T$ equally spaced intervals over the cycle to obtain,

$$\mathbf{w_{hb}} = \begin{pmatrix} \mathbf{w(t_0 + \Delta t)} \\ \mathbf{w(t_0 + 2\Delta t)} \\ \vdots \\ \mathbf{w(t_0 + T)} \end{pmatrix} \qquad \mathbf{R_{hb}} = \begin{pmatrix} \mathbf{R(t_0 + \Delta t)} \\ \mathbf{R(t_0 + 2\Delta t)} \\ \vdots \\ \mathbf{R(t_0 + T)} \end{pmatrix}, \tag{7}$$

where $T$ is the period of the cycle and $\Delta t = 2\pi/(N_T \omega)$. The vectors in Eq. (7) are then combined with Eq. (6) using a transformation matrix $\mathbf{E}$ to relate the vector of Fourier coefficients to the respective HB vector. Introducing a matrix $\mathbf{D} = \mathbf{E^{-1}AE}$, this can then be reduced to

$$\omega \mathbf{D} \mathbf{w_{hb}} + \mathbf{R_{hb}} = \mathbf{0}. \tag{8}$$

Equation (8) is solved by introducing a pseudo-time derivative to allow iteration to convergence using a time-domain CFD solver,

$$\frac{\mathrm{d}\mathbf{w_{hb}}}{\mathrm{d}\tau} + \omega \mathbf{D} \mathbf{w_{hb}} + \mathbf{R_{hb}} = \mathbf{0}. \tag{9}$$

Equation (9) only differs from Eq. (1) by the HB source term $\omega \mathbf{D} \mathbf{w_{hb}}$. The treatment of this source term is a key concern for effective solution of the HB system. An explicit treatment of this term can lead to instabilities for certain problems although a method to stabilise this was presented in Custer (2009). An alternative is to include the source term in the Jacobian matrix to form a fully implicit system as presented in Woodgate and Badcock (2009). The linear system that must be solved for the implicit time stepping to the solution of Eq. (9) is real, has Jacobian terms of the residual at each time slice retained for the Harmonic Balance solution on the diagonal of a blocked matrix, and has these blocks linked through diagonal blocks. The fully implicit approach is the one used in this work. Once a converged solution is reached, the $\mathbf{w_{hb}}$ vector contains the flow solution at a number of discrete points around the cycle. Once the Fourier coefficients are known, the time domain solution is reconstructed using Eq. (5).

### 2.3. *Implicit CFD solver*

The solution of the systems arising in the frequency domain methods is carried out in this paper using two CFD solvers. The LFD method uses the implicit solvers within the DLR TAU code (Gerhold (1997)). The Jacobians used for the preconditioners are formed analytically with either a first order or second order stencil depending on the spatial discretisation required. The HB method is run using the fully implicit CFD solver PMB (Badcock *et al.* (2000), Woodgate and Badcock (2009)). The terms in the residual are calculated using Osher's approximate Riemann solver with MUSCL interpolation to obtain second order accuracy combined with a turbulence model for the viscous contributions in RANS simulations. For both methods, linear systems of the form $\mathbf{Ax} = \mathbf{b}$ are set up, allowing solution with a generalised conjugate residual (GCR) Krylov subspace method (Eisenstat *et al.* (1983)) with incomplete lower-upper preconditioning (Saad (2000)).

## 3. Solving Linear Systems

Using implicit solvers requires the solution of a linear system of the form $\mathbf{Ax} = \mathbf{b}$. For CFD analyses, the matrix $\mathbf{A}$ can be very large and often poorly conditioned. There is a need for efficient preconditioning particularly for very stiff or non-diagonally dominant systems. For the LFD method, an iterative preconditioned Krylov subspace solver has been used. Methods of preconditioning have been the focus of a number of papers summarised in Benzi (2002). The majority of the techniques when applied to CFD problems are primarily focussed on using properties of the given matrix to carry out the permutation of terms to improve the conditioning. Very few papers make use of properties of the underlying problem to improve the preconditioner performance. In Pueyo and Zingg (1997), Wong and Zingg (2005), the preconditioner is based upon an approximate Jacobian matrix and is shown to accelerate the convergence compared with using the exact Jacobian. This work makes use of approximate Jacobians to significantly accelerate the solution of linear systems arising from the CFD derived LFD problem.

Preconditioning looks to improve the condition number of a matrix in order to make a system easier to solve using an iterative method. A linear system of the form

$$\mathbf{Ax} = \mathbf{b} \tag{10}$$

is recast, for left preconditioning, as

$$\mathbf{P^{-1}Ax} = \mathbf{P^{-1}b} \tag{11}$$

An incomplete lower-upper (ILU) factorisation can be used to form an approximation to the inverse by limiting the number of additional non-zero terms introduced beyond the original sparsity pattern during the factorisation process described in Saad (2000). This is referred to as ILU($k$) preconditioning where $k$ indicates the level of fill-in. In the current work one level of fill-in is used, which generates around two additional non-zero terms in the matrix for each original non-zero term.

For CFD applications, a Jacobian matrix $\mathbf{A_2}$ based on the second-order spatial discretisation, is often found to lead to a very poor preconditioner $\mathbf{P}$ in the sense of bad convergence of the Krylov method. This was shown in Chow and Saad (1997) that for non-symmetric non-diagonally dominant matrices, the incomplete factors can be more ill conditioned than the original matrix. It is possible to view this effect by assessing how well the preconditioner approximates the matrix $\mathbf{A^{-1}}$ from looking at the solution of $\mathbf{Px} = \mathbf{b}$. If the preconditioner was obtained using a direct method (i.e. $\mathbf{P^{-1}} \equiv \mathbf{A^{-1}}$), the exact solution would result. However, as an incomplete factorisation is used, the preconditioner is only an approximation (i.e. $\mathbf{P^{-1}} \approx \mathbf{A^{-1}}$). The exact solution and second order preconditioner solution are shown in Fig. 1.

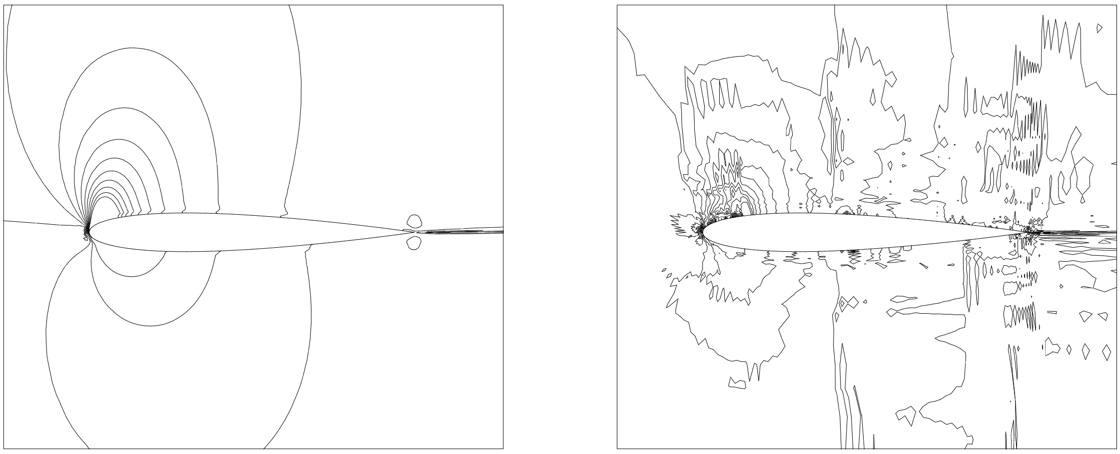

(a) Exact solution **Ax=b** (b) **Px=b**

Figure 1. Second order preconditioner comparison

It can be seen that the preconditioner based on the pure second order spatial discretisation gives a solution which is highly oscillatory. This is consistent with poor convergence of the Krylov method. Similar unstable behaviour in the forward and backward solves were shown in Elman (1986) and Bruaset *et al.* (1990). A heuristic fix is to base $\mathbf{P}$ on the Jacobian matrix $\mathbf{A_1}$ of the first-order spatial scheme, which seems to improve on this situation significantly. This has the benefit of being more stable due to the increased diagonal dominance as was shown in Saad (1994). The solution of the first order preconditioner is shown in Fig. 2.

The preconditioner based on the first order Jacobian has little oscillatory behaviour and is a reasonable approximation to the exact solution. This is due to the better conditioning of the first order Jacobian not causing any stability problems in the factorisation steps for forming the preconditioner. A variation on this approach is to calculate $\mathbf{P}$ based on the matrix $\mathbf{A}_\alpha$, where

$$\mathbf{A}_\alpha = \alpha\mathbf{A_2} + (\mathbf{1} - \alpha)\mathbf{A_1} \tag{12}$$

The weighted preconditioner matrix $\mathbf{P}_\alpha$ is then formed from the ILU factorisation of the

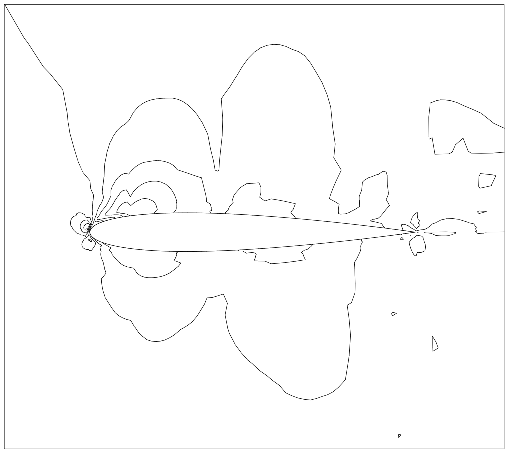

Figure 2. First order preconditioner

matrix $\mathbf{A}_{\alpha}$. The solution of the new weighted preconditioner is shown in Fig. 3.

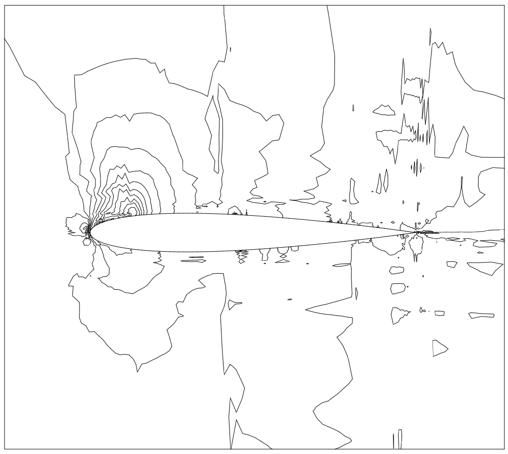

Figure 3. Weighted preconditioner $\alpha = 0.90$

For $\alpha = 0.90$, the majority of the small oscillations seen in Fig. 1(b) have been damped by the introduction of a small amount of the first order Jacobian terms. The improved stability in the factorisation and the better approximation from the second order terms would be expected to improve the convergence of the linear solver.

The weighted preconditioner $\mathrm{ILU}_{\alpha}$ has been implemented for the solution of the linear systems arising in the LFD method using a restarted GCR Krylov subspace solver (Eisenstat *et al.* (1983)). It is necessary to understand what effect the $\mathrm{ILU}_{\alpha}$ preconditioning has on the convergence of the system and look to what happens to the solution when this preconditioner is used. Results are shown here for the NACA 0012 aerofoil in forced pitch, with the flow modelled by the Euler equations.

For assessing the performance of the new preconditioner, a sweep of $\alpha$ values for $0 \leq \alpha \leq 1$ is carried out. A NACA 0012 aerofoil has been used with 31,416 points at AGARD CT2 conditions (Landon (1982)), maximum iteration count of 2000 and a minimum residual of $1\text{x}10^{-8}$ with 20 Krylov subspace vectors. The $\alpha$ sweep is shown in Fig.4(a) for both left and right preconditioning with one level of fill-in in the ILU factorisation.

Figure 4(a) shows that as the parameter $\alpha$ is increased from zero (preconditioned based on pure first-order discretisation), the number of iterations to convergence reduces

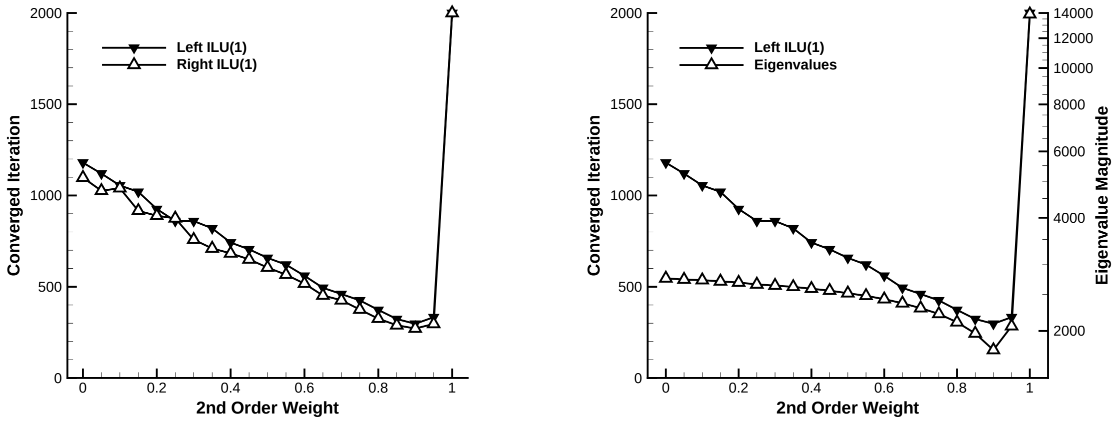


(a) Iterations for convergence (b) Convergence and Eigenvalue magnitude

Figure 4. NACA 0012 AGARD CT2 results

down to around a factor of 5 fewer at $\alpha = 0.90$. However, the solver does not converge for $\alpha = 1.0$ (preconditioner based on the pure second-order discretisation). Similar behaviour has been observed for a wide variety of cases (insviscid and viscous aerofoil problems, inviscid and viscous wings and full aircraft configurations).

Further assessment is shown in Fig. 4(b). This shows the magnitude of the largest eigenvalue of the preconditioner matrices at different values of $\alpha$ as an indication of conditioning of the matrix. Eigenvalues closer to the origin indicate a better conditioned matrix. In this figure, it can be seen that as the number of iterations for convergence improves, the magnitude of the largest eigenvalue reduces (i.e. becomes closer to the origin). The blending of terms from the better conditioned first-order Jacobian matrix and the better approximation from the second-order Jacobian matrix clearly improves the overall effectiveness of the preconditioner.

## 4. Applications

A number of works have been carried out applying Fourier based methods to both Aeroelastic and Flight Dynamics problems.

### 4.1. *Aeroelasticity*

Numerical approaches are routinely used to assist in flight flutter testing where traditionally linear aerodynamic models are predominantly discussed due to cost considerations. Aeroelastic stability analysis looks at the growth and decay of the system response following an infinitesimal excitation. As such, the LFD approach is a well suited simplification of the fully nonlinear aerodynamic system.

Taking the modal form of the structural equations and linearising using the assumption of small perturbations gives the aeroelastic eigenvalue problem for the stability analysis as,

$$\left\{\lambda_j^2\mathbf{M_u} + \lambda_\mathbf{j}\mathbf{C_u} + \mathbf{K_u}\right\}\mathbf{\hat{u}_j} = \mathbf{\Phi^T}\frac{\partial \mathbf{f}}{\partial \mathbf{u}}\mathbf{\hat{u}_j} + \mathbf{\Phi^T}\frac{\partial \mathbf{f}}{\partial \mathbf{w}}\mathbf{\hat{w}_j}. \tag{13}$$

where $\mathbf{M_u}$, $\mathbf{C_u}$ and $\mathbf{K_u}$ are the matrices of modal mass, damping and stiffness of dimensions $n \times n$ with $n$ as the number of normal modes, $\mathbf{\Phi}$ is the mode shape matrix, $\mathbf{\hat{u}}_j$ is the complex amplitude of a small structural perturbation (i.e. an eigenvector) and $\lambda_j$ is the corresponding eigenvalue, the imaginary part of which gives the circular frequency $\omega_j$. Additionally, the vector of generalised aerodynamic forces is written as $\mathbf{\Phi^T}\mathbf{\hat{f}} = \mathbf{Q}(\mathbf{k})\mathbf{\hat{u}_j}$. The matrix $\mathbf{Q}$ contains the aerodynamic influence coefficients depending on the reduced frequency $k$ as dimensionless form of the circular frequency.

The additional unknown vector $\mathbf{\hat{w}}_j$ for the fluid is modelled using the expression given in Eq. (3), which results in the aeroelastic eigenvalue problem,

$$\left\{\lambda_j^2\mathbf{M_u} + \lambda_\mathbf{j}\mathbf{C_u} + \mathbf{K_u}\right\}\mathbf{\hat{u}_j} = \mathbf{Q}\mathbf{\hat{u}_j} \tag{14}$$

where,

$$\mathbf{Q} = \mathbf{\Phi^T}\left\{\frac{\partial \mathbf{f}}{\partial \mathbf{u}} - \frac{\partial \mathbf{f}}{\partial \mathbf{w}}\left(\mathbf{i}\omega_\mathbf{j}\mathbf{I} + \frac{\partial \mathbf{R}}{\partial \mathbf{w}}\right)^{-1}\left(\frac{\partial \mathbf{R}}{\partial \mathbf{u}} + \mathbf{i}\omega_\mathbf{j}\frac{\partial \mathbf{R}}{\partial \mathbf{\dot{u}}}\right)\right\}. \tag{15}$$

To avoid expensive repeated computation of the aerodynamic influence matrix, it is pre–computed for a small number of frequencies dictated by the normal mode frequencies using the LFD solver. Kriging interpolation applied to these pre–computed values makes the CFD approach similar to conventional linear aerodynamic tools as discussed in Timme *et al.* (2011).

Figure 5 shows results of a typical stability analysis of the Goland wing/store configuration (see Badcock *et al.* (2011) for details). The damping ratio and the frequency are given as a function of the equivalent airspeed. The reference results were computed solving Eq. (15) repeatedly, using the complex frequency $\lambda_j$, when solving the aeroelastic eigenvalue problem (which is costly but possible). The mode traces computed using kriging interpolation for the aerodynamic influence matrix are in excellent agreement with the reference prediction. The Goland wing/store configuration encounters the classical wing–bending–torsion flutter mechanism with interacting low frequency bending and torsion modes. The interaction of the two higher frequency modes of this configuration results in a second instability at a higher value of equivalent airspeed.

This case required 196 solves to evaluate the variation of the aerodynamic influence to establish the flutter boundary for each Mach number in this range. LFD is at least an order of magnitude quicker (2.7 times the computational cost of a steady-state for this case) than the equivalent time-accurate solve, showing the benefit of using the frequency domain methods for this application. As the number of solves required scales with the number of points in the parameter range (e.g. frequency), number of parameters and the number of normal modes, it is clear that the use of a time-accurate solver is no longer feasible and the use of frequency domain methods combined with an effective sampling technique is even more important. Other cases that have been computed with this method include several aerofoils, the MDO wing and the open source fighter aircraft configuration, all described in Badcock *et al.* (2011), and a RANS computation of a large realistic aircraft model based on 100 normal modes.

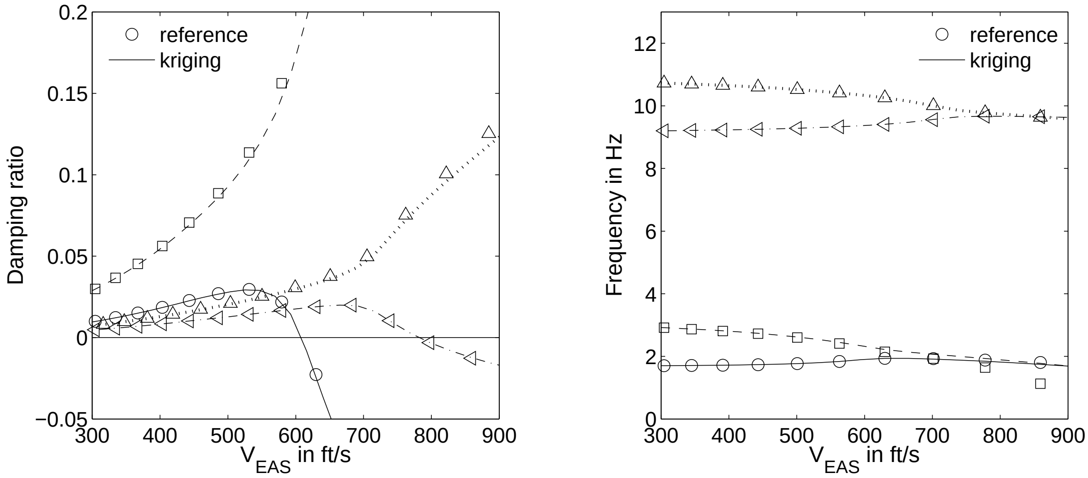


(a) Damping ratio

(b) Frequency in Hz

Figure 5. Damping ratio and frequency vs. equivalent airspeed (VEAS) for Goland wing/store configuration.

The linear solver for each case typically accounts for around 90% of the solution time. The rest of which is spent setting up the relevant matrices. The benefit to having an improved linear solver is clear.

## 4.2. *Dynamic Derivatives*

For flight dynamics analysis, force and moment dependency on flight and control states is often expressed in tabular form. An efficient method for the generation of aerodynamic tables using CFD was reported in Da Ronch *et al.* (2011a). These tables are typically formed from static data and require dynamic derivatives to introduce the effects from an unsteady motion. Previous studies have looked at exploiting frequency domain methods for the generation of the dynamic derivative terms in Da Ronch *et al.* (2011b), benchmarking these against the time-accurate solve.

Dynamic derivatives are computed from forced periodic oscillations. The computation of the longitudinal dynamic derivative values from the time-histories of the forces and moments assumes that the aerodynamic coefficients are linear functions of the angle of attack, $\alpha$, pitching angular velocity, $q$, and rates, $\dot{\alpha}$ and $\dot{q}$. The in-phase and out-of-phase components of the measured or computed aerodynamic loads are defined as

$$\bar{C}_{j_\alpha} = \left(C_{j_\alpha} - k^2\, C_{j_{\dot{q}}}\right) \tag{16}$$

$$\bar{C}_{j_q} = \left(C_{j_{\dot{\alpha}}} + C_{j_q}\right) \tag{17}$$

for $j = L, m, D$. In Da Ronch *et al.* (2012), two techniques to post-process time-domain sampled data arising from forced applied motions have been described to obtain the values of these dynamic terms.

To assess the frequency domain methods, a two-dimensional NACA 0012 aerofoil was run at AGARD CT2 conditions (Landon (1982)) with a time-accurate solver, the LFD solver and Harmonic Balance with 1, 2 and 3 modes retained. Figure 6 shows the response of the pitching moment coefficient to the changing instantaneous angle of attack. Increasing the number of Fourier modes in the HB solution had little effect on the result after the first three modes. Observe that including the second Fourier mode in the HB solution has a large impact on improving the correlation to the reference solution. This reflects the frequency spectrum of the moment coefficient, due to the flow conditions and symmetry in the aerofoil geometry. Higher modes are not included, but they closely overlap the reference solution. The LFD solution is illustrated in Fig. 6(b), and indicates a degraded prediction of the moment dynamic dependence. Consistent with the other data, the LFD predicts a large hysteresis but the loop has a lower mean slope than the other methods.

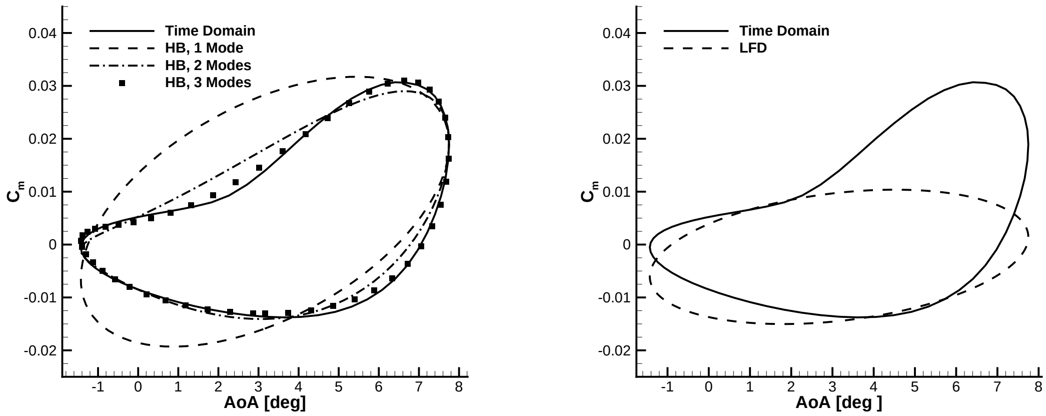


(a) Pitching moment coefficient, HB (b) Pitching moment coefficient, LFD

Figure 6. NACA 0012: pitching moment coefficients dynamic dependence ($M = 0.6$, $\alpha_0 = 3.16°$, $\alpha_A = 4.59°$, and $k = 0.0811$)

The force and moment loops indicate the accuracy of the dynamic derivatives values. For the pitching moment, the HB results illustrate that the one-mode solution should provide a reasonable estimation of the information needed for flight dynamics although for greater accuracy, at least two modes would be required. The predictions of the LFD should be reasonable for the aerodynamic damping term (i.e. loop hysterisis), while the in-phase component would feature a large inaccuracy (i.e. gradient of mean slope). This case is however, outside of the assumptions made to formulate the LFD solver and as such would be expected.

While providing adequate predictions, the main benefit of the frequency domain methods is the computational savings that can be obtained. Figure 7 conveys the computational efficiency of the HB method with respect to the underlying time-domain simulation (line corresponding to a speed up = 1). For the comparison, the solutions were obtained using 64 time-steps per cycle and were simulated for 3 periods.

The LFD solution was obtained with a speed up of around 60 compared to the corresponding time-domain solver where the LFD solve is 0.82 times the steady-state cost for this case. While achieving the largest computational time saving, a loss in accuracy was observed in the LFD-based predictions of dynamic derivatives. With a performance of a similar order to the LFD method, the HB formulation was seen to be adequate for the prediction of stability characteristics and local flow variables. By retaining more Fourier modes, the HB method eventually loses favour relative to solving the time-dependent equations although for the majority of cases, low numbers of harmonics are used.

The frequency domain methods have also previously been applied to other models for

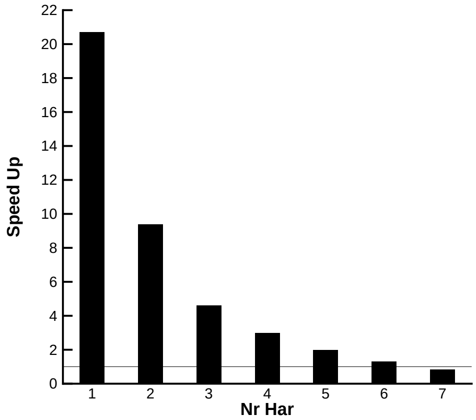


Figure 7. CPU time speedup for Harmonic Balance method

flight dynamics purposes such as the SDM generic fighter aircraft in Da Ronch *et al.* (2011b), for the DLR-F12 transport aircraft configuration in Da Ronch (2012) and for the transonic cruiser configuration.

The dynamic derivative model presented here is widely used although there are key regimes where it is no longer adequate such as when history effects and non-linearities begin to dominate. Previous work by the authors along with continuing work is making use of frequency domain methods to assess this model.

As for the aeroelastic application, a considerable amount of the solution time is spent in the linear solver. For the HB method, this is around 95% due to the increased stiffness of the matrices. Again, having a way to accelerate the convergence of the linear solver is of great benefit for this application.

## 5. Conclusions

The LFD and Harmonic Balance methods have been demonstrated for flutter and dynamic derivative calculations, with sample results shown in this paper typical of a much larger set of cases that have previously been published. The key issue for obtaining the maximum computational gain from using the frequency domain formulation is the ability to solve linear systems efficiently. The key challenge in this is the formation of an effective preconditioner. Using ILU to form the preconditioner based on the Jacobian matrix of the second order spatial discretisation (which is the Jacobian of the problem we are interested in) results in very poor convergence of a Krylov method. It has been found that adding a small proportion of the first order spatial scheme Jacobian before preconditioning effectively remedies this situation. Results presented in section 3 suggest that the iterative process associated with forward and backward substitution is unstable for the second order Jacobian, and that adding the first order Jacobian helps with this. A rigorous analysis of this problem would require the identification of a suitable model problem that is tractable.

The performance of the linear solver was considered in the context of two applications, flutter analysis and dynamic derivative calculation. The LFD solver is the ideal tool for the linear flutter analysis, providing high computational efficiency to allow routine calculations of the stability based on very large models. A recent study of an in-production aircraft case, using 35 million grid points for a RANS flow model, 100 structural modes, and retaining the full geometrical complexity of the aircraft, resulted in the damping-air speed plots being generated at the rate of 1 Mach number per day using an 800 core supercomputer. This calculation was not optimised, and it is likely that this time can be reduced. The key to this level of performance is in the efficiency of the LFD solver, in turn relying on the linear solver. The disadvantage of LFD is the inability to predict nonlinear effects such as LCO. This can be tackled by the HB solver, or through a nonlinear model reduction technique which uses the coupled system eigenvectors as a basis (Badcock *et al.* (2011)). The latter approach has the possible advantage of providing a more feasible method for gust load analysis and control law design.

For the calculation of dynamic derivatives, it was found that the results of time domain calculations could be reproduced using a number of modes in the HB solution, and that there were significant discrepancies with the LFD solution. This is mainly due to the fact that the LFD solver calculates solutions from the steady state flow field, whereas the HB solver mean state is the time averaged solution over the cycle that introduces some knowledge of the shock motion over the cycle. On the face of it the HB is useful for this application. However, it should be noted that the right context for assessing whether the HB offers significant improvements over LFD is in the influence that these have on the final flight dynamics analysis. In this context the assumption of dynamic derivatives, such as the independence on frequency of the applied motion, and the neglection of dependence on several other parameters, must also be considered. For demanding flow conditions, involving moving shocks, separation and vortices, it is possible that these assumptions are not valid, and will be as least as significant as the effect of including nonlinearity in the frequency domain solution. This subject is the matter of further study.

## Acknowledgements

The work of the first author was supported by the Engineering and Physical Sciences Research Council and Airbus.

## References

Badcock, K.J., Richards, B., and Woodgate, M., 2000. Elements of Computational Fluid Dynamics on Block Structured Grids Using Implicit Solvers. *Progress in Aerospace Sciences*, 31 (5-6), 351–392.

Badcock, K.J., *et al.*, 2011. Transonic aeroelastic simulation for instability searches and uncertainty analysis. *Progress in Aerospace Sciences*, 47 (5), 392–423.

Benzi, M., 2002. Preconditioning Techniques for Large Linear Systems: A Survey. *Journal of Computational Physics*, 182 (2), 418–477.

Bruaset, A.M., Tveito, A., and Winther, R., 1990. On the Stability of Relaxed Incomplete LU Factorizations. *Mathematics of Computation*, 54, 701–719.

Chow, E. and Saad, Y., Experimental Study of ILU Preconditioners for Indefinite Matrices. , 1997. , Technical report UMSI 97/95, Supercomputing Institute, University of Minnesota.

Custer, C.H., 2009. A Nonlinear Harmonic Balance Solver for an Implicit CFD Code: OVERFLOW 2. Thesis (PhD). Department of Mechanical Engineering and Materials Science, Duke University.

Da Ronch, A., 2012. On the Calculation of Dynamic Derivatives Using Computational Fluid Dynamics. Thesis (PhD). School of Engineering, University of Liverpool, Liverpool, U.K.

Da Ronch, A., Ghoreyshi, M., and Badcock, K.J., 2011a. On the generation of flight dynamics aerodynamic tables by computational fluid dynamics. *Progress in Aerospace Sciences*, 47 (8), 597–620 Special Issue - Modeling and Simulating Aircraft Stability and Control.

Da Ronch, A., *et al.*, 2011b. Linear Frequency Domain and Harmonic Balance Predictions of Dynamic Derivatives. *Submitted to Journal of Aircraft* See also AIAA 2010-4699.

Da Ronch, A., *et al.*, 2012. Evaluation of Dynamic Derivatives Using Computational Fluid Dynamics. *AIAA Journal*, 50 (2), 470–484.

Eisenstat, S.C., Elman, S.C., and Schultz, M., 1983. Variational Iterative Methods for Nonsymmetric Systems of Linear Equations. *SIAM, Journal of Numerical Analysis*, 20 (2), 345–357.

Elman, H.C., 1986. A Stability Analysis of Incomplete LU Factorizations. *Mathematics of Computation*, 47, 191–217.

Gerhold, T., 1997. Calculation of Complex Three-Dimensional Configurations Employing the DLR TAU-Code. *In*: *35th AIAA Aerospace Sciences Meeting and Exhibit*, January., Reno,NV.

Hall, K. and Crawley, E., 1989. Calculation of Unsteady Flows in Turbomachinery Using the Linearized Euler Equations. *AIAA Journal*, 27 (6), 777–787.

Hall, K., Thomas, J., and Clark, W., 2002. Computation of Unsteady Nonlinear Flows in Cascades Using a Harmonic Balance Technique. *AIAA Journal*, 40 (5), 879–886.

He, L. and Ning, W., 1998. Efficient Approach for Analysis of Unsteady Viscous Flows in Turbomachines. *AIAA Journal*, 36 (11), 2005–2012.

Landon, R.H., AGARD R-702 Compendium of Unsteady Aerodynamic Measurements. , 1982. , Technical report, Advisory Group for Aerospace Research and Development - NATO.

McMullen, M., Jameson, A., and Alonso, J., 2006. Demonstration of Nonlinear Frequency Domain Methods. *AIAA Journal*, 44 (7), 1428–1435.

Mialon, B., *et al.*, 2011. Validation of Numerical Prediction of Dynamic Derivatives: The DLR-F12 and the Transcruiser Test Cases. *Progress in Aerospace Sciences*, 47 (8), 674–694.

Mortchelewicz, G., Application des équations d'Euler linéarisées à la prévision du flottement. , 1998. , Technical report AGARD R-822, AGARD.

Murman, S., 2007. Reduced-Frequency Approach for Calculating Dynamic Derivatives. *AIAA Journal*, 45 (6), 1161–1168.

Pueyo, A. and Zingg, D., 1997. Progress in Newton-Krylov Methods for Aerodynamic Calculations. *In*: *AIAA 35th Aerospace Sciences Meeting and Exhibit*, AIAA-97-0877, 6-9 January., Reno, NV.

Saad, Y., 2000. *Iterative Methods for Sparse Linear Systems 2nd edition*. Self Published.

Saad, Y., 1994. Krylov Subspace Techniques, Conjugate Gradients, Preconditioning and Sparse Matrix Solvers. *In*: *Von Karman Institute for Fluid Dynamics Lecture Series 1994-05*, March.

Thomas, J., Dowell, E., and Hall, K., 2002. Nonlinear Inviscid Aerodynamic Effects on Transonic Divergence, Flutter, and Limit-Cycle Oscillations. *AIAA Journal*, 40 (4), 638–646.

Thomas, J., Dowell, E., and Hall, K., 2004. Modeling Viscous Transonic Limit-Cycle Oscillation Behaviour Using a Harmonic Balance Approach. *Journal of Aircraft*, 41

(6), 1266–1274.

Timme, S., Marques, S., and Badcock, K.J., 2011. Transonic aeroelastic stability analysis using a kriging–based Schur complement formulation. *AIAA Journal*, 49 (6), 1202–1213.

Wong, P. and Zingg, D., 2005. Three-Dimensional Aerodynamic Computations on Unstructured Grids Using a Newton-Krylov Approach. *In*: *17th AIAA Computational Fluid Dynamics Conference*, AIAA-05-5231, 6-9 June., Toronto, Canada.

Woodgate, M. and Badcock, K.J., 2009. Implicit Harmonic Balance Solver for Transonic Flow with Forced Motions. *AIAA Journal*, 47 (4), 893–901.